Physical Science International Journal
4(5): 657-668, 2014

SCIENCEDOMAIN *international*
www.sciencedomain.org

Evidence for Negative Electron Affinity in Laser Irradiated ZnTe Thin Films

Sachin D. Kshirsagar[1,2] and M. Ghanashyam Krishna[1,2*]

[1]Advanced Centre of Research in High Energy Materials, University of Hyderabad, Hyderabad-500046, India.
[2]School of Physics, University of Hyderabad, Hyderabad-500046, India.

Authors' contributions

This work was carried out in collaboration between both authors. The first author SDK carried out the experiments which were designed jointly by the authors SDK and MGK. The paper was also written jointly by both authors. Both authors read and approved the final manuscript.

Original Research Article

Received 9th July 2013
Accepted 28th September 2013
Published 5th February 2014

ABSTRACT

Local transport properties of laser irradiated ZnTe thin films are reported. By rastering the laser beam (of 532 nm wavelength) appropriately, ZnTe decomposes into *n*-type ZnTe and Te and a grating like structure with micro-stripes of ZnTe separated by grooves of Te is obtained. Conductive atomic force microscopy studies and local I-V measurements made on the stripes and grooves show that the film properties are mainly determined by chemical composition, rather than by the topography of the film. When the tip is positively biased, the current images closely match the topography images. In contrast, when the tip is negatively biased the current and topography images are very different and a large negative current was also observed in the grooves. This is attributed to the variation in charge separation (interface capacitance) caused by the rough surface. It is shown that Te forms ohmic contact with Au tip, but the junction exhibits Schottky diode behavior under low biasing voltages. The large current at both high positive and negative tip biasing may arise due to semi-metallic properties of Te. The I-V characteristics measurement reveals formation of Schottky barrier between ZnTe-Au junctions with a very low value (32.4 – 78.3 meV) of barrier which indicates the presence of negative electron affinity.

*Corresponding author: Email: mgksp@uohyd.ernet.in;

Keywords: ZnTe films; conducting atomic force microscopy; metal/semiconductor interface; Schottky Barrier.

1. INTRODUCTION

In semiconductors with negative electron affinity (NEA), the vacuum level lies below the conduction-band minimum. Hence, an electron excited into the conduction band has enough energy to leave the semiconductor surface. Semiconductors with NEA provide an alternative way to achieve low work function materials because the Fermi level can be tailored by band gap engineering. There has been intensive effort in the search for new materials with NEA. Diamond like carbon (DLC) is a promising material due to its low electron affinity [1]. Unfortunately, the applications of DLC are limited because of its metastable nature. As a result, other materials such as III-V compound semiconductors have been extensively studied for this purpose [2]. ZnTe is an II-VI semiconductor that intrinsically shows *p*-type conduction and has a 2.26 eV band gap [3-5]. Semiconductors with low band gap energy and low electron affinity are vital for the design of cold-cathode electron emitters employed in field emitters and flat-panel displays [6]. Since, electron affinity is defined as the difference between the vacuum level and the conduction-band minimum, it can be correlated with band gap of semiconductor by the following relation [7]

$$\chi = I - E_g \quad (I)$$

where E_g is band gap energy, χ is electron affinity, and I is ionization energy

Therefore, in the present work the possibility of NEA in an II-VI semiconductor, ZnTe, is investigated. Laser irradiation of ZnTe films causes dissociation in to ZnTe and Te which is expected to lead to the formation of Te deficient ZnTe showing *n*-type conduction and decrease in band gap. Since the variations in transport properties will occur locally, i.e. within grains and grain boundaries, the electrical properties of laser treated ZnTe thin films have been investigated using the technique of conductive atomic force microscopy (CAFM). CAFM also provides the possibility to investigate breakdown phenomena on a nanometer scale. In the present case, CAFM results showed that the distribution of low and high current carrying regions is largely decided by chemical composition at metal-semiconductor interface rather than topographic features of semiconductor surface. The influence of laser annealing on surface morphology and optical properties are also reported. To the best of the current authors' knowledge there are no other studies on the possibility of NEA in ZnTe thin films.

2. EXPERIMENTAL DETAILS

Thin films of ZnTe were deposited on borosilicate glass substrate by electron beam evaporation technique in high vacuum (<5 x 10^{-6} Torr). The thickness of the films measured using a stylus profilometer [XP-1 of Ambios, USA] was of the order of 1000 nm. The films were subjected to laser irradiation at a wavelength of 532 nm and power of 40 mW. To makes stripes on the surface, the film was raster scanned in a plane perpendicular to the laser beam axis using a linear XY sample stage. The scan table can be set to produce alternate uneven x-y oscillation. With the laser beam being focused, the film is moved relative to beam position using a computer-controlled piezoelectric stage. The rastering of the tightly focused laser beam produces melting and redistribution of ablated material and consequently the line pattern on the surface. The continuous motion of the film prevents

complete melting at the focal point of the laser beam. Note that films to be rastered were not fixed with the sample stage. Due to uneven x-y motion, the sample placed on the piezoelectric stage is slightly displaced from original position, so rastering is repeated on a comparatively larger area. Repeating the auto scan cycle for up to 12 hrs ensures patterning of film. The pattern consisted of set of vertical long stripes connected by short horizontal lines, making them easy to locate in the CAFM. The dimension of stripes estimated from SEM and AFM analysis is about 5 micron with approximate spacing of 1 micron.

Spectral transmittance curves were recorded in a UV-Vis-NIR spectrophotometer (Model V570 of JASCO, Japan) scanning in the range 190-2500 nm. The structural properties of the films before and after laser annealing were determined by means of Grazing incidence x-ray diffraction (GI-XRD) (Bruker D8 Discover diffractometer and Cu K_α radiation (λ=1.5405A^o)) with a grazing angle of 1.5º. The surface morphology of the ZnTe films was investigated by Field emission Scanning Electron Microscope (FE-SEM Ultra55 of Carl Zeiss), combined with an Energy dispersive X ray analysis (EDX) probe, using an electron beam energy of 10 to 20 keV. Prior to investigation, all the films were coated with a uniform Au layer for good electrical conductivity. EDX analyses were performed to identify the elemental composition.

The Conductive-Atomic Force Microscopy (C-AFM) studies were carried out in a SPI 3800 probe station (SII Inc., Japan) designed to perform topographical and conductivity measurements, simultaneously. The C-AFM was operated in the constant force contact mode with Si cantilevers. The tip and one side of the cantilever were coated with 25 nm Au layer and its radius of curvature is less than 35 nm. The sample stage and the cantilever are carefully insulated from the apparatus frame. The other electrode was formed by the conductive silver paint pasted on the top surface of the films, to which a bias voltage was applied. The conductive tip was the counter microelectrode, connected to the ground potential. The current (I) images were simultaneously measured by applying a bias voltage (V) in the range of ± 10 V and maximum current ±100 nA. Note that no reliable current image could be obtained below a bias voltage of ± 4 V. I–V curves were plotted by averaging data of ten independent scans, each scan was separated by 100 msec delay time. Current measurements were also performed by changing direction of bias voltage. Pt films of ~ 40 nm deposited by RF magnetron sputtering onto undoped single crystal Si substrates were used as standard reference samples.

3. RESULTS AND DISCUSSION

3.1 Structure and Microstructure

The X-ray diffraction pattern for the as-deposited ZnTe thin film in Fig. 1(a) reveals that the films are a mixture of amorphous and microcrystalline phases as evidenced by the broad peaks centering around 25 and 45º. However, on subjecting the films to laser irradiation there is an amorphous-crystalline transition, as seen from Fig. 1(b). Majority of the observed peaks can be assigned to the zinc blende phase of ZnTe (PCPDF file no. 89-3054). In addition to these, there are peaks which are attributed to elemental Te (PCPDF file no. 89-4899) at 2θ values of 27.4º and 38.3º. Laser irradiation, thus, not only causes crystallization of the films but also the dissociation of ZnTe in to ZnTe and Te.

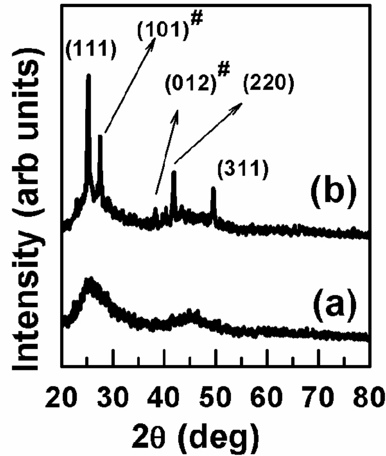

Fig. 1. XRD patterns of (a) as deposited and (b) laser treated ZnTe thin films (# indicates Te phase)

The surface morphology of the laser treated ZnTe film observed under the FE-SEM at different magnifications is shown in Fig. 2(a)-(d). The chemical composition of the films examined using EDX confirmed that the all films are Te-rich. The surface has a hierarchical microstructure with a top layer consisting of clusters of particles that are between 100-300 nm in size. Underneath the clusters are micron sized stripes of material (referred to as the plateau region in the rest of the paper) separated by grooves (referred to as the valley region in the rest of the paper) patterned over a large area that appear like gratings. The area of the image in Fig. 2(a) is roughly 100 x 100 μm^2 and the width of the each strip is 2 to 4 µm with an inter-strip separation between 100-200 nm. Higher magnification image in Fig. 2(b) shows that within the stripes there is a further hierarchy of microstructures with micron sized clusters below which there are further layers of materials. Further magnification of these areas in Figs. 2(c) and (d) reveals the formation of nano-clusters within the stripes. It is generally accepted that higher contrast will result from larger band gap (here ZnTe) material while lesser contrast will result from low band gap (here Te) material due to the difference in ionization energy of the low and high band gap materials [8].

By comparing color contrast in secondary electron images (Fig. 2(a),(b)), it can be inferred that there is a difference in chemical composition between the area within the stripes and the grooves. Similar studies on ZnTe crystals were reported in the literature by Yabe *et al.* [9].

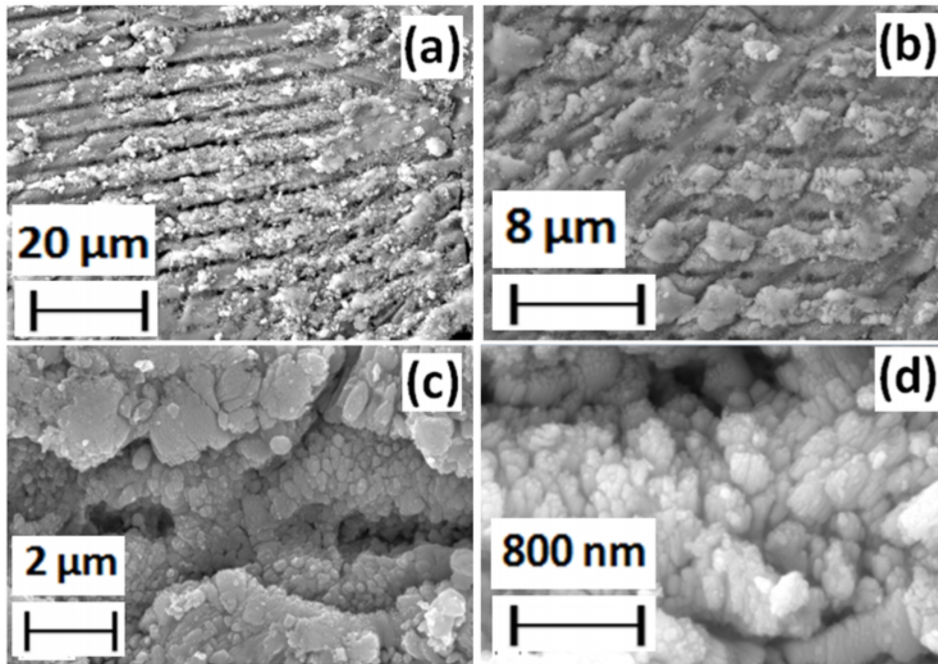

Fig. 2. Scanning electron micrographs of laser treated ZnTe thin films with increasing magnification and (a) 20 μm, (b) 8 μm, (c) 2μm and (d) 800 nm scale bars

3.2 Optical Transmittance

The measured spectral transmission curve of the as-deposited ZnTe films is shown in Fig. 3. It shows interference fringes due to the refractive index contrast between the film and substrate. The transmission in the long wavelength region above the band gap is > 80%. The fringe height is wavelength dependent, indicating optical inhomogeneity [10]. The refractive index derived from the measured spectral transmission curves [5] varies between 2.9 to 3.1 in the wavelength region between 1100 to 2500 nm, indicating a slight dispersion as a consequence of the optical inhomogeneity. The laser annealed films showed lower refractive index as compared to the as-deposited ZnTe thin films which can be attributed to the increase free carrier absorption. The band gap has been calculated by extrapolating linear portion of the Tauc plot to the energy axis [5]. The band gap value for the as-deposited and laser treated films are 1.4 eV and 1.2 eV, respectively.

The optical band gap is less than the value of 2.26 eV for bulk ZnTe [11]. The spectral transmission of the films decreased by more than 15% under the influence of the laser irradiation and this was accompanied by a red-shift in the band gap which could be attributed to the formation of structural defects in laser treated films sample that leads to formation of energy states near the band edges. The detailed investigation on optical properties will be presented elsewhere.

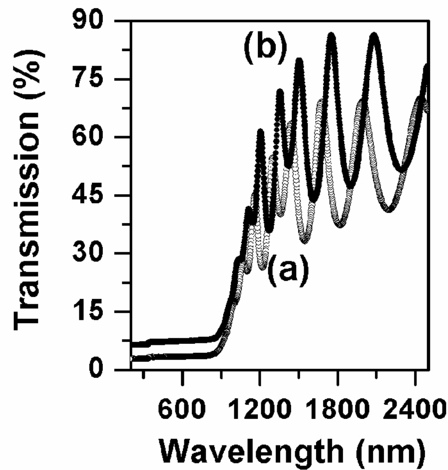

Fig. 3. Optical transmission spectra of (a) as deposited and (b) laser treated ZnTe thin films

3.3 Topography and Current Images

The typical topography and current map recorded under ambient conditions are shown in Fig. 4. The topography images in Fig. 4 and the current maps in Fig. 5 were recorded simultaneously using a C-AFM while applying a bias voltage varying between ±10 V. In the current images, the bright regions correspond to high current carrying domains and the dark regions to low current carrying domains. The distribution of the bright spots is concentrated on the plateau region while low conductivity area is mostly centered in the valley region. The topography and current images reveals rough surface (as high as 400 nm) and inhomogeneous transport properties. Te is possibly segregated in the grooves created due to the dissociation and crystallization process.

Significantly, thermal annealing of ZnTe at 500°C also causes dissociation of ZnTe into ZnTe and Te. Hence, it is reasonable to assume that ZnTe crystallization and nucleation may form Te deficient (*n*-type) ZnTe. The nucleation characteristics of Te are different due to large difference in melting point of ZnTe (1239°C) and Te (449°C). It is, therefore, concluded that at elevated temperature the Te formed a '*liquid-like'* phase which drifts to the valley region of the film resulting in Te segregation.

To obtain detailed information of the ZnTe and Te distribution in laser treated portion, C-AFM images were correlated with topography images. Fig. 5 (a) and (b) show the current images obtained using positive tip bias. Note that, although the current images show good correlation with topography images, the variation in conductivity does not only result from variation in topography. As discussed above, the plateau region is made up of *n*-type (Te deficient) ZnTe while the valley region is made up of Te segregates. The current image of the film shows that there is pattern of conducting stripes (plateau region) surrounded by relatively insulating stripes (valley region). A similar pattern can also be seen in SEM images (Fig. 2 (a) and (b)). The electrical contrast clearly provides evidence for phase separation in current images. The valley region (dark features) consists mainly of Te segregates which form ohmic contact with the Au tip. High conductivity (bright) regions were also observed

and these are assigned to *n*-type ZnTe phase. Interestingly, when the tip was biased with -4 V (Fig. 5(c)), no correlation was observed between the current and topography images. Also, the reverse contrast was not observed when tip was negatively biased indicating non-significant role of positive charge (holes) carriers from the film.

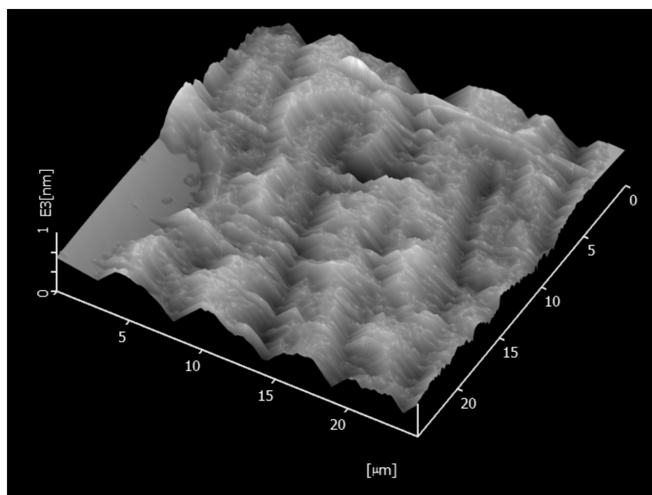

Fig. 4. Continuous three-dimensional topography images of the laser treated ZnTe thin films

Notably, significant increase in current was observed (Fig. 5(d)) in the valley region with increase in bias voltage, a result possibly related to the semimetal properties of Te [12]. Since the current maps showed significant variation with polarity of tip biasing, formation of Schottky barrier at Au-Te interface cannot be ruled out. On the other hand, as seen in Fig. 5(c) and (d), there is no morphological correlation to the electric current images in the (ZnTe-Au junction) plateau region of the film. This distinction is a direct consequence of the fact that a Schottky diode is a majority carrier device. The leakage current during reverse bias is, therefore, very small. The strong breakdown can only produce large reverse current which was not observed up to -10 V in most of the films. However, an extremely low leakage current at high applied reverse voltage can be attributed to minimal recombination across the barrier. It is worth noting that the current images, when the tip was biased with negative potential, show that the currents flow through some portions of the valley region attaining negative values. The origin of negative current is probably the variation in charge separation caused by the rough (rms value 400 nm) surface. Due to the resistive electrical contact, upon contact with a metal, charging of the semiconductor surface is expected. The deposited charge may spread over a region that is much larger than the size of the contact [13]. A metal tip deposits electrons on the semiconductor surface, so that the local charge density rises until an equilibrium potential is achieved. The deposited charges are in proportion to the applied reverse bias voltage and charge separation. The movement of tip over the rough semiconductor surface produces a variation in charge separation. The increase of charge separation reduces electrostatic force acting on the carriers which, in turn, tends to drift carriers in the opposite direction to maintain equilibrium, producing negative current. To get more insight into the difference in the electric transport between the plateau and valley regions, local I-V measurements were carried out, as discussed in the following section.

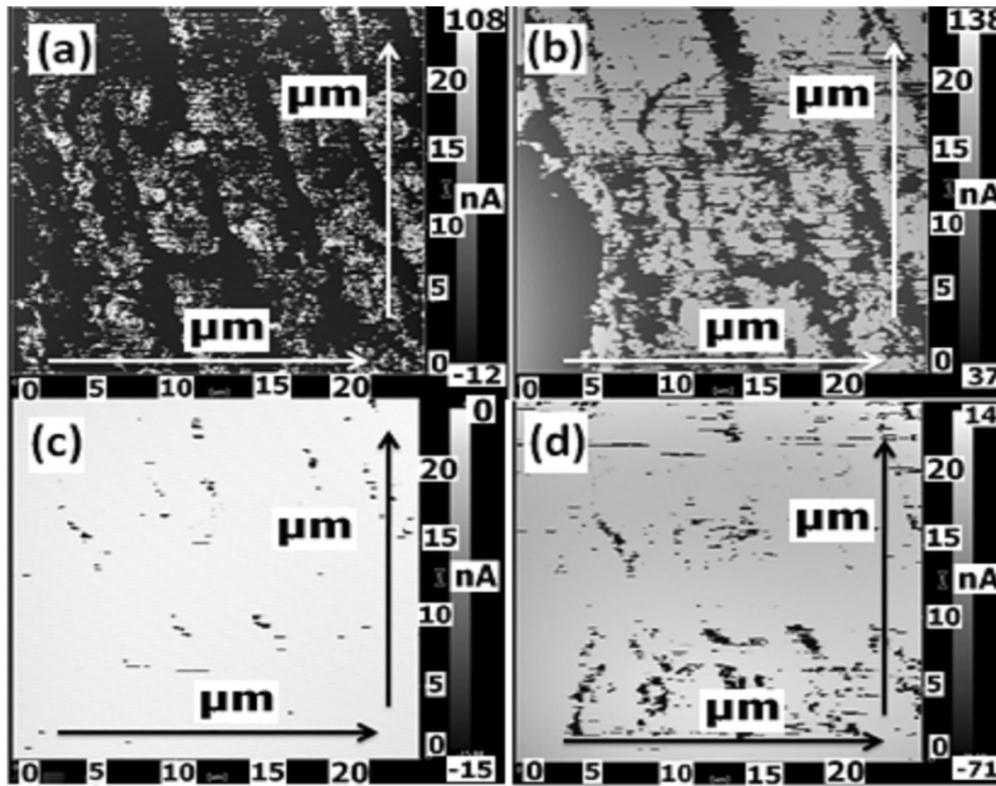

Fig. 5. Continuous two-dimensional current images of laser treated ZnTe films. The tip bias voltage was (a) +4 V, (b) +7 V, (c) -4 V and (d) -7 V. The contrast from white to black corresponds to the variation of current from 100 nA to -100 nA

3.4 I-V Measurements

I-V measurements were carried out on the plateau and valley regions of the film surface. The current values from I-V curves can be compared with the corresponding current images in Fig. 5. Fig. 6(a) shows the measured I-V characteristics for the Au-Te junction (valley region).

From the figure, it is evident that the contacts do not display complete ohmic properties even though they exhibit almost symmetrical characteristics under positive and negative tip bias. Some deviation in I-V curves was observed when tip bias was ramped from +5 to 0 V and 0 to -5 V, indicating Schottky diode like behavior. The observed behavior suggests that under high bias conditions, the Au-Te junction no longer exists and the characteristics transform from Schottky barrier to ohmic contact type of behavior. It is well known that the difference in work function between metal tip and sample is crucial to determine the direction and amount of flow of current. In general, electrons flow from a material with low work function to a material with high work function. It is also expected that the currents across the metal-semiconductor (M-S) interface will be decided by the type of majority charge carriers. The junction may behave like an ohmic or rectifying contact depending on the combination of metal and semiconductor used. In the present study, Au coated tip has a work function (i.e. electron affinity for metals) of ≈5.1 eV, as compared to the electron affinity of Te of ≈4.95 eV

[14]. Thus, I-V properties of the Au-Te junction can be attributed to the small difference in Au and Te electron affinities, low (0.3 eV) band gap [15] and semi-metallic properties of Te [12]. The semi-metallic properties of Au-Te junction deduced from the present I –V measurements are in good agreement with the microscopic analysis of the valley regions inferred by the CAFM images. These observations support the observation that the valley region in Fig. 4 is comprised of Te segregates. Thus, the most likely origin of the Schottky barrier might be the small mismatch in work function of Au and Te and intrinsic *p*-type conduction in semiconducting Te [15].

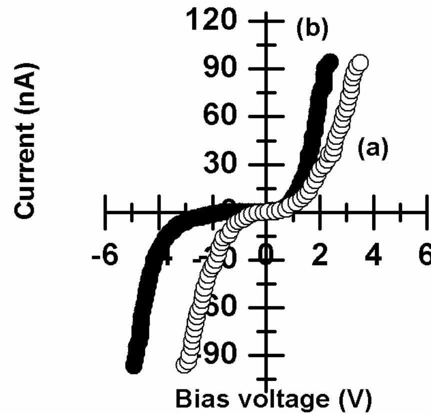

Fig. 6. The I-V characteristics of (a) Au-Te and (b) Au-ZnTe junction of laser treated ZnTe film

As shown in Fig. 6(b), when the tip bias is swept from +5 V to 0 V, the ZnTe-Au junction draws very large current indicating a situation similar to that of the forward bias condition of a diode. It should be noted that ZnTe has higher work function (5.27 eV) [16] than the Au-tip (5.1 eV) [14] suggesting that electron flow in the junction should encounter maximum resistance when ZnTe is negatively biased (i.e. tip is positively biased). This leads to the conclusion that ZnTe acts as an electron source indicating *n*-type nature, which is inconsistent with conventionally observed intrinsic *p*-type conduction in ZnTe (i.e. current in ZnTe is governed by the electrons instead of holes). The inference can be justified by the fact that dissociation of ZnTe into ZnTe and Te leads to the formation of Te deficient (*n*-type) ZnTe. It should be noted that in Te deficient ZnTe (leading to *n*-type ZnTe), defects will form which, in turn, can cause decrease in the work function of *n*-type ZnTe. As discussed in the analysis of transmittance, the band gap of ZnTe decreased because of its non-stoichiometry and formation of defect states. The large deviation from bulk band gap value of ZnTe might be also related to the decrease in work function of laser treated ZnTe [17-18]. Further, it was also seen that when voltage is swept from 0 V to -5 V, there was sharp decrease in current showing rectifying behavior. Since the nature of contact between M-S junction not only depends on the type of majority charge carriers in semiconductor but also on work functions of metal and semiconductors, a semiconductor with *n*-type conduction will form a rectifying contact only with a metal of high work function, indicating large decrease in work function of ZnTe [19].

According to the Schottky–Mott model, barrier height is given by the difference between metal work function and electron affinity of the semiconductor [20]. It has also been proved that in compound semiconductors barrier height changes with the band gap variations [21-

22]. In I-V measurements, as the reverse bias across MS junction is increased, a Fowler-Nordheim type tunneling current would be observed. The Fowler-Nordheim current (I_{FN}) can be expressed as:

$$I_{FN} = A\alpha \frac{V^2}{t^2} exp\left[-\beta \frac{t}{V}\right] \quad \text{(II)}$$

where *A* is the effective emission area (35 nm) of the conducting probe, *V* is applied voltage, *t* is thickness (1500 nm with roughness 400 nm) of the *n*-type ZnTe. α and β are given by

$$\alpha = \left[\frac{q^3 m}{8\pi h m^* \phi}\right] \text{and } \beta = \left[\frac{4(2m^*)^{1/2}\phi^{3/2}}{3\hbar q}\right] \quad \text{(III)}$$

Here *m* is the free-space electron mass, *q* is the electron charge, *h* is Planck's constant, *m** (=0.09 m) is the effective mass of electron in ZnTe [23]. In the current study, barrier height was determined by plotting $In\left(\frac{J}{E^2}\right)$ verses $\frac{1}{E}$, where $J = \frac{I_{FA}}{A}$ and $E = \frac{V}{t}$. It is observed that the plot (Fig. 7) is a straight line whose slope is (-β). The estimated value of barrier height is 32.4 – 78.3 meV.

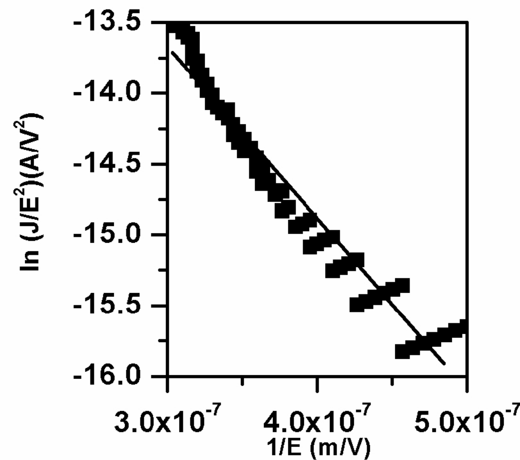

Fig. 7. The Fowler–Nordheim plots for current–voltage characteristics measured on the Au-ZnTe junction

Before concluding we would like to stress that thickness of *n*-type ZnTe (conducting region only) in present case must differ from the estimated thickness of thin film due to high roughness and composite nature of material. Although there might be significant deviation in actual value of barrier height, the extremely low value is very significant. This extremely low value of barrier height will facilitate further studies, particularly of the intrinsic *n*-type doping, which, in turn, may provide more physical insight for development of M-S junction detector for high frequency (THz) signals [24].

Thus, based on I–V analysis it is clear that Schottky diode-like properties were observed at the Au-ZnTe interface and there is *n*-type conduction in ZnTe indicating significant reduction

of work function of non-stoichiometric ZnTe. Thus, the present results clearly demonstrate the existence of negative electron affinity in Te deficient ZnTe achieved by modifying band gap and work function of ZnTe.

4. CONCLUSIONS

The influence of 532 nm wavelength laser irradiation on the electrical transport properties, measured by conductive atomic force microscopy (C-AFM), of electron beam evaporated ZnTe thin films is reported. The as deposited films are a mixture of amorphous and microcrystalline phases and transformed to the crystalline state accompanied by dissociation of ZnTe into ZnTe and Te under influence of the laser treatment. Dissociation of ZnTe leads to formation of Te deficient ZnTe causing inversion of its conductivity to *n* type. The results of scanning electron microscopy (SEM) and atomic force microscopy (AFM) topography images revealed that the laser treatment forms long stripe like structures containing valley and plateau regions. The brightness and electrical contrast in SEM and current images, respectively, clearly indicates phase separation. The current–voltage (I-V) analysis and current maps indicated that the valley regions mainly consisted of Te segregates while the plateau regions are comprised of *n*-type ZnTe. The formation of a Schottky barrier at the Au-ZnTe junction was clearly demonstrated. The very low value (32.4 – 78.3 meV) of barrier height offers great prospect for development of high frequency detectors. Transport properties at the Au-Te interface can be interpreted in terms of the combined effect of semi-metallic properties of Te and formation of Schottky diode. The results provide evidence for negative electron affinity in laser treated ZnTe thin films.

ACKNOWLEDGEMENT

The authors acknowledge the facilities provided by the School of Physics. Dr D S Kothari Fellowship for SDK is also acknowledged.

COMPETING INTERESTS

Authors have declared that no competing interests exist.

REFERENCES

1. Lmimouni K, Legrand C, Dufour C, Chapoton A, Belouet C. Diamond-like carbon films as electron-injection layer in organic light. Appl. Phys. Lett. 2001;78:2437.
2. Machuca F, Liu Z, Maldonado JR, Coyle ST, Pianetta P, Pease RFW. Negative electron affinity group III-nitride photocathode demonstrated as a high performance electron source. J. Vac. Sci. Technol. B. 2004;22:3565.
3. Tanaka T, Guo Q, Nishio M, Ogawa H. Characterization of Al-doped ZnTe layer using scanning capacitance microscopy and Kelvin probe force microscopy. J. Phys.: Conf. Ser. 2007;61:1162.
4. Amassian A, Dudek M, Zabeida O, Gujrathi SC, Klemberg-Sapieha JE, Martinu L. Oxygen incorporation and charge donor activation via subplantation during growth of indium tin oxide films. J. Vac. Sci. Technol. A. 2009;27:362.
5. Kiran MSRN, Kshirsagar S, Krishna MG, Tewari SP. Structural, optical and nanomechanical properties of (111) oriented nanocrystalline ZnTe thin films. Eur. Phys. J. Appl. Phys. 2010;51:10502.

6. Cahay M, Boolchand P, Fairchild SB, Grazulis L, Murray PT, Back TC. Rare-earth monosulfides as durable and efficient cold cathodes. J. Vac. Sci. Technol. B. 2011;29:602.
7. Wills JM, Alouani M, Andersson P, Delin A, Eriksson O, Grechnyev O. Full-Potential Electronic Structure Method: Energy and Force Calculations. 1st ed. Berlin: Springer; 2010.
8. Wu J, Cao J, Han W, Janotti A, Kim H. Functional Metal Oxide Nanostructures. 1st ed. London: Springer; 2012.
9. Yabe T, Asahi T, Sato K. Reduction of Te inclusions in ZnTe single crystals by thermal annealing. Phys. Stat. Sol. C. 2004;1:921-24.
10. Uma Mahendra Kumar K, Brahma R, Krishna MG, Bhatnagar AK, Dalba G. An optical study of Ni induced crystallization of a-Si thin films. J. Phys.: Condens. Matter. 2007;19:496208.
11. Oda O. Compound semiconductor bulk materials and characterizations. 1st ed. Tokyo: World Scientific; 2007.
12. Bouroushian M. Electrochemistry of Metal Chalcogenides. 1st ed. Berlin: Springer; 2010.
13. Cui XD, Zarate X, Tomfohr J, Primak A, Moore AL, Moore TA, et al. Bias-induced forces in conducting atomic force microscopy and contact charging of organic monolayers. Ultramicroscopy. 2002;92:67.
14. Haynes W M. CRC Handbook of Chemistry and Physics. 91st ed. Boca Raton: CRC; 2011.
15. Corbett JW. Electron radiation damage in semiconductors and metals. 1st ed. New York: Academic Press; 1966.
16. Triboulet R, Siffert P. CdTe and Related Compounds; Physics, Defects, Hetero- and Nano-structures, Crystal Growth, Surfaces and Applications. 1st ed. Oxford: Elsevier; 2009.
17. Monch W. Schottky contacts on ternary compound semiconductors: Compositional variations of barrier heights. Appl. Phys. Lett. 1995;67:2209.
18. Monch W. Empirical tight-binding calculation of the branch-point energy of the continuum of interface-induced gap states. J. Appl. Phys. 1996;80:5076.
19. Goswami A. Thin Film Fundamentals. 1st ed. New Delhi: New Age International; 2007.
20. Rhoderick EH, Williams RH. Metal-Semiconductor Contacts. 2nd ed. Oxford: Clarendon; 1988.
21. Chyi JI, Shieh JL, Lin RJ, Pan JW, Lin RM. Schottky barrier heights of $In_xAl_{1-x}As$ ($0 \le x \le 0.35$) epilayers on GaAs. J. Appl. Phys. 1995;77:1813.
22. Lin CL, Chu P, Kellner AL, Wieder HH. Composition dependence of $Au/In_xAl_{1-x}As$ Schottky barrier heights. Appl. Phys. Lett. 1986;49:1593.
23. Hayashi S, Sanda H, Agata M, Yamamoto K. Resonant Raman scattering from ZnTe microcrystals: Evidence for quantum size effects. Phys. Rev. B. 1989;40:5544.
24. Shashkin V, Chechenin Y, Danil'tsev V, Khrykin O, Maslovsky A, Murel A, et al. Planar Schottky Diodes with Low Barrier Height for Microwave Detector Application. IEEE MIEL Microelectronics. 2002;1:335.

© 2014 Kshirsagar and Krishna; This is an Open Access article distributed under the terms of the Creative Commons Attribution License (http://creativecommons.org/licenses/by/3.0), which permits unrestricted use, distribution, and reproduction in any medium, provided the original work is properly cited.

Peer-review history:
The peer review history for this paper can be accessed here:
http://www.sciencedomain.org/review-history.php?iid=428&id=33&aid=3549